Proceedings of the International Conference on Nanotechnology: Fundamentals and Applications
Ottawa, Ontario, Canada, 4-6 August 2010
Paper No. 451

Frequency Analysis of Single-Walled Carbon using a Structural Mechanics Approach

V. Parvaneh, M. Shariati, H. Torabi
Shahrood University of Technology, Department of Mechanical Engineering
Daneshgah Blvd, shahrood, Semnan, Iran
Member of the Young Researchers Club of Azad University of Mashhad
Vali.Parvaneh@gmail.com; mshariati44@gmail.com; torabi.mech87@gmail.com

ABSTRACT

This paper develops a structural mechanic model that analyzes the natural frequency of single-walled carbon nanotubes (SWCNTs) subjected to fixed-fixed and free-fixed boundary conditions. The necessity of desirable conditions and expensive tests for experimental methods, in addition to the time expenditure required for atomic simulations, are the motivation for this work. Because the present model is constructed in the CAE space of ABAQUS, there is no need to program for different loading and boundary conditions. A Morse potential is employed for stretching and bending potentials, and a periodic type of bond torsion is used for torsion interactions. The natural frequencies for various aspect ratios are predicted by this structural model. The effect of different vacancy defects on the natural frequency of zigzag and armchair nanotubes is also investigated. These findings are in good agreement with the existing numerical results.

1 INTRODUCTION

The discovery of carbon nanotubes by Iijima (1991) opened up a new window in nanoscience. An extremely high stiffness and light weight in CNTs results in high vibration frequencies. Due to these features, the vibrational behavior of CNTs is a fundamental characteristic that should be fully studied because it is essential for applications such as NEMS devices. Gibson et al. (2007) studied the vibrational behavior of CNTs and their composites, including both theoretical and experimental studies. Kwon et al. (2005) used eigenvalue analysis of mass and stiffness matrices computed from atomistic simulations and predicted the natural frequencies and mode shapes of various carbon nanotubes. Xu et al. (2008) studied the free vibration of double-walled CNTs modeled as two individual beams by considering van der Waals interactions between the inner and outer tubes. Their methods can mainly compute the bending modes of the vibrational modes and natural frequencies. S.K. Georgantzinos and N.K. Anifantis (2009) reported a study of the vibrational characteristics of multi-walled carbon nanotubes modeled exclusively using springs and lumped masses. They examined the effects of different constraints at the nanotube ends on the computed frequencies and mode shapes. By investigating the influence of van der Waals interactions, they concluded that the presence of all corresponding elements is necessary in the vibration analysis of MWCNTs.

Here, we studied frequency analysis of fixed–fixed and free-fixed SWCNTs with different aspect ratios (L/D) and compared their frequencies with those of numerical methods. Therefore in this work structural mechanics model (Parvaneh et al., 2009) is employed to determine the natural frequencies and their corresponding modes for two types of SWCNTs i.e., zigzag and armchair.

2 CARBON NANOTUBE MODELLING

A single-walled carbon nanotube can be considered as a rolled graphene sheet so that the direction of rotation determines the type of nanotube (zigzag, armchair, or chiral). Various interactions exist between the carbon atoms in constitutive carbon nanotubes. The motions of carbon atoms are regulated by a force field that is generated by electron-nucleus interactions and nucleus-nucleus interactions, which can be expressed in the form of steric potential energy. The total steric potential energy is the sum of energies due to interactions between carbon atoms (Rappe et al., 1992):

$$u_{total} = u_r + u_\theta + u_\phi + u_\omega + u_{vdw} + u_{el} \quad (1)$$

where u_r, u_θ, u_ϕ, and u_ω are bond energies associated with bond stretching, angle variation or bond bending, dihedral angle torsion, and out-of-plane torsion, respectively and u_{vdw} and u_{el} are also non-bonded energies associated with Van der Waals and electrostatic interactions, respectively. For prediction of behavior of nanotubes under axial tensional load, we can apply other potentials in lieu of stretching and bending potentials. However, we do not allow potentials apart from torsion potential and out-of-plane torsion potentials for the analysis of buckling.

$$u_{total} = u_r + u_\theta + u_\phi + u_\omega \tag{2}$$

Different expressions have been developed for these potentials. Brenner and Morse potentials are well-known and are the usual potentials applied to nanotubes. The Brenner potential function is more accurate and more versatile than the Morse potential; however, it is also more complex. In this paper, Morse potentials are employed for stretching and bending potentials, and a periodic type of bond torsion is applied for torsion and out-of-plane torsion interactions (Eqs. (3)-(6)). The parameters at these potentials are listed in Table 1(Cornell et al., 1995).

$$u_r = D_e\left\{ \left[1-e^{-\beta(r-r_0)} \right]^2 - 1 \right\} \tag{3}$$

$$u_\theta = \frac{1}{2}k_\theta(\theta-\theta_0)^2\left[1+k_{sextic}(\theta-\theta_0)^4 \right] \tag{4}$$

$$u_\phi = \frac{1}{2}k_\phi\left[1+\cos(n\phi-\phi_0) \right] \tag{5}$$

$$u_\omega = \frac{1}{2}k_\omega\left[1+\cos(n\omega-\omega_0) \right] \tag{6}$$

As indicated in Fig. 1(a) and Fig. 2, a nonlinear axial spring is used for modeling of the angle variation interaction between atoms. The relationship between changes in the bond and the corresponding change in length of the spring for small displacements can be expressed simply by Eq. 7 (Odegard et al., 2002).

$$\Delta\theta \approx \frac{2(\Delta R)}{r_0}, r_0 = 0.142nm \tag{7}$$

Therefore, we can simplify equation (6) to equation (8).

$$u_\theta = \frac{2}{r_0^2}k_\theta(R-R_0)^2\left[1+\frac{16}{r_0^4}k_{sextic}(R-R_0)^4 \right] \tag{8}$$

The stretch force, the angle variation moment, the dihedral angle torque, and out-of-plane torque can be obtained from differentiations of (Eqs. (3), (8), (5), (6)) as functions of bond stretch, bond angle, dihedral angle, and out-of-plane angle variation, respectively:

$$F(r-r_0) = 2\beta D_e\left[1-e^{-\beta(r-r_0)} \right] e^{-\beta(r-r_0)} \tag{9}$$

$$F(R-R_0) = \frac{4}{r_0^2}k_\theta(R-R_0)\left[1+\frac{16}{r_0^4}(1+\frac{4}{r_0^2})k_{sextic}(R-R_0)^4 \right] \tag{10}$$

$$T(\phi-\phi_0) = \frac{1}{2}k_\phi n\sin(n\phi-\phi_0) \tag{11}$$

$$T(\omega-\omega_0) = \frac{1}{2}k_\omega n\sin(n\omega-\omega_0) \tag{12}$$

In the present structural model, interactions between atoms are modeled with spring and connector elements so that the carbon atoms are joint points. A nonlinear connector is considered for modeling of the stretching and torsional interactions and a nonlinear spring for modeling of the angle variation interaction (see Fig. 2).

Carbon atoms in ABAQUS are modeled by a discrete rigid sphere so that connector elements between toms are adjoined to reference points at the center of the sphere and a local coordinate is set at the center of each atom. This local coordinate is a combination of a Cartesian coordinate for stretching and a rotational coordinate for torsion. The X direction of these coordinates is in the connector direction, and the Z direction is vertical to the central axis of the nanotube. Because we can only use a linear spring in the CAE space of

ABAQUS, by changing the linear spring command to a nonlinear spring command in the input file, and by applying the nonlinear data for F(ΔR) versus ΔR using Eq. 10, we can apply the bond bending spring to the model. For applying bond stretch and torsion forces to the connectors, we can apply the nonlinear stiffnesses in three directions (X,Y,Z) directly. For stretching stiffness in the X direction, we can obtain the nonlinear data for F(Δr) versus Δr by Eq. 9, and for torsional stiffness in X direction, we can obtain the nonlinear data for T($\Delta\phi$) versus $\Delta\phi$ by Eq. 11. For torsional stiffness in the Y direction, we can obtain the nonlinear data for T($\Delta\omega$) versus $\Delta\omega$ by Eq. 12.

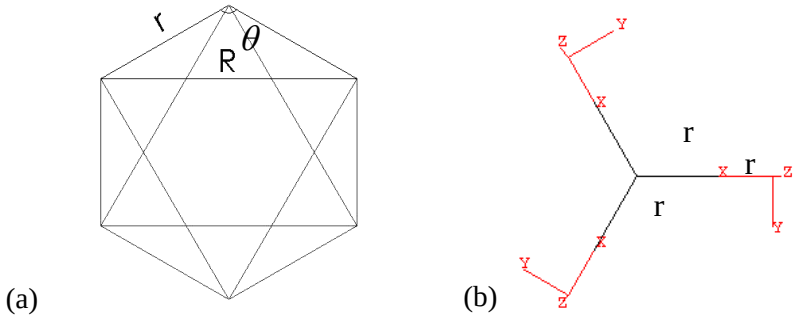

Fig. 1: (a) A hexagonal unit cell, (b) Location of local coordinates of each connector

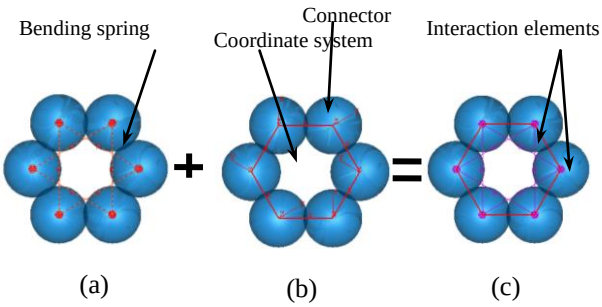

Fig. 2: Spring and connector elements corresponding to the interactions of carbon atoms. (a) The angle variation interactions, (b) the stretching and torsional interactions, (c) total interactions.

3 RESULTS AND DISCUSSION

In this section, the commercial finite element numerical package ABAQUS is applied to study the natural frequency of a fixed-fixed and free-fixed SWCNT. The natural frequencies were predicted by the present structural model. Zigzag (12,0) and armchair (7,7) SWNTs with various aspect ratios (L/D) were employed for this study. The effect of different types of defects on the natural frequency is also studied for zigzag and armchair nanotubes with various aspect ratios. Fig. 3 shows the natural frequencies of perfect and defective nanotubes with different aspect ratios. The natural frequencies are obtained by our present model, and are compared with results from K.Hashemnia et al. (2009). As indicated in Fig. 2, the vacancy defects have a very weak effect on the natural frequencies when the Euler mode occurs. Of course, it should be noted that for defective nanotubes, the Euler mode will happen later; it occurs at an aspect ratio of approximately 5 for a single vacancy defect.

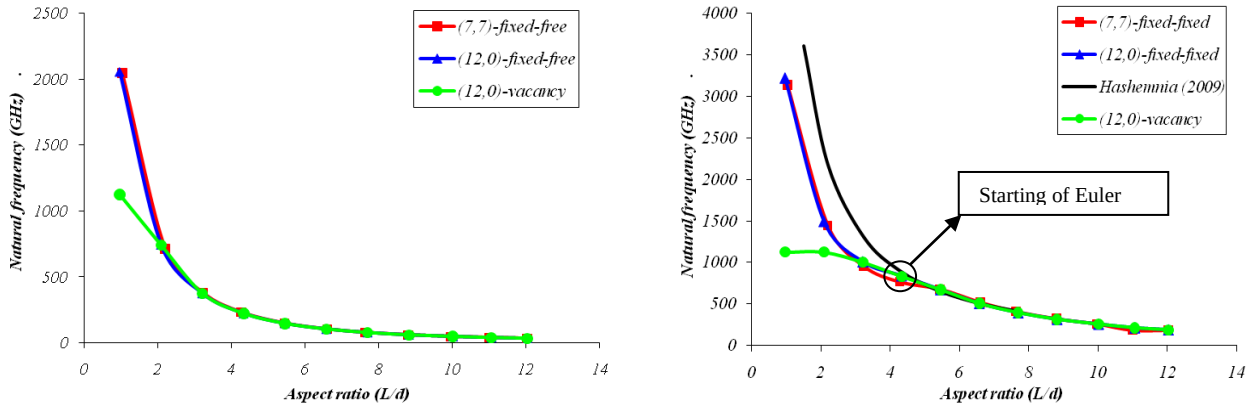

(a) (b)

Fig. 2: Natural frequencies vs. aspect ratio of SWCNTs with (a) fixed-free and (b) fixed-fixed boundary conditions.

When the Euler buckling mode occurs (aspect ratio of up to 5), the natural frequency follows from the analytical equations. Therefore, we can calculate the natural frequency by the analytical equation simply enough for the long carbon nanotubes. Also, we have compared the present results to those from the simple continuum model. The value of the effective thickness for the nanotube is adopted as 0.066 nm (Yakobson et al., (1996)). This proposed value provided excellent results for the critical strain, but the effective thickness t = 0.066 nm could not be used when studying buckling load from the critical strain, because the cross-section of a CNT can only be expressed by A = pdt, where t = 0.34 nm is to be applied. However, with an effective wall thickness of 0.34 nm for CNTs, we can not model these by continuum shell models because the Euler mode will happen much earlier. There may be an equivalent wall thickness for the continuum shell model that predicts the critical buckling load and corresponding mode shapes correctly.

As a conclusion, it can be seen that the results of this continuum model are in acceptable agreement with the present model for nanotubes with diameter of d=0.95 nm and various lengths. This agreement is better for long nanotubes than short nanotubes (high aspect ratios).

The mode shapes according to the displacement contours are represented for various lengths of zigzag nanotubes in Fig. 4. With increasing aspect ratio of nanotubes, the shell mode shapes convert to the Euler mode shape.

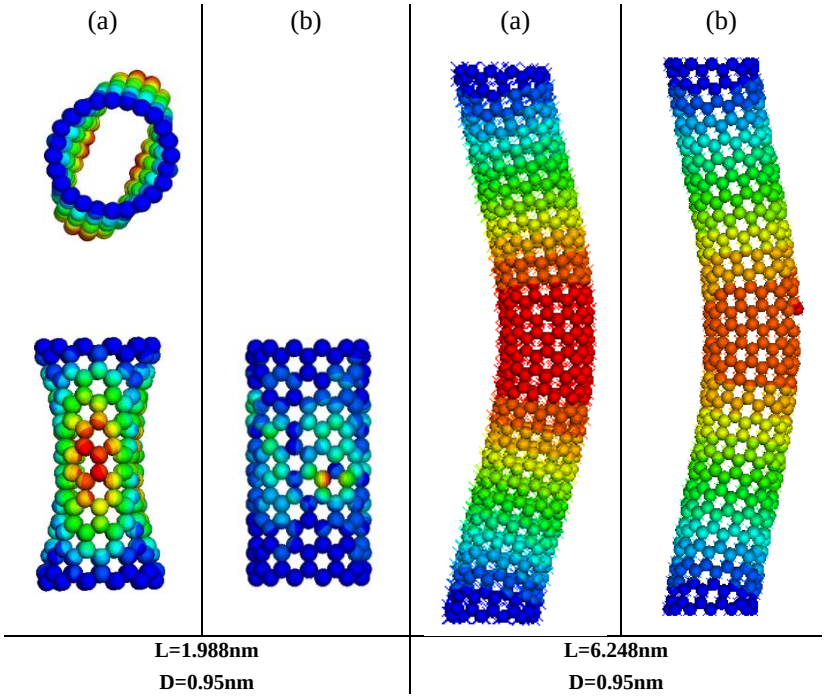

Fig. 4: The mode shapes of (12,0) SWCNTs under frequency analysis (a) perfect and (b) defective.

4 CONCLUSION

In the present paper, SWCNTs with particular fixed-fixed and free-fixed boundary conditions under frequency analysis were studied based on a structural mechanics approach using ABAQUS. From our findings, the following conclusions can be drawn:

1. With increasing aspect ratio of nanotubes, the shell mode shapes convert to the Euler mode shape.
2. Tube chirality has not a significant effect on the natural frequency of SWCNTs.
3. The vacancy defects have a significant effect on the natural frequency when shell modes occur.
4. The vacancy defects cause the Euler mode to occur later.

REFERENCES

Cornell W.D., Cieplak P., Bayly C.I., et al. (1995). A second generation force-field for the simulation of proteins, nucleic-acids, and organic-molecules. Journal of American Chemical Society 117, 5179–5197.

Georgantzinos S.K., Giannopoulos G.I., Anifantis N.K. (2009). Vibration analysis of multi-walled carbon nanotubes using a spring–mass based finite element model, Computational Mechanics, 43, 731–741.

Gibson R.F., Ayorinde E.O., Weng Y. (2007). Vibrations of carbon nanotubes and their composites: A review ,Composites Science and Technology, 67, 1–28.

Hashemnia K., Farid M., Vatankhah R. (2009). Vibrational analysis of carbon nanotubes and grapheme sheets using molecular structural mechanics approach. Computational materials science 47, 79-85

Iijima S. (1991). Helical microtubes of graphitic .carbon Nature, 354, 56–58**.**

Kwon Y.W., Mathena C., Oh J.J., Srivastava D. (2005). Vibrational characteristics of carbon nanotubes as nanomechanical resonators, Journal of Nanoscience and Nanotechnology, 5, 703–712.

Odegard, G.M., Gates, T.S., Nicholson, L.M., Wise, K.E., 2002. Equivalent-continuum modeling with application to carbon nanotubes. NASA/TM-2002-211454.

Parvaneh V., Shariati M., Majd Sabeti A.M. (2009). Investigation of defects effects on the buckling behavior of SWCNTs via a structural mechanics approach, European Journal of Mechanics A/Solid, 28, 1072–1078.

Rappe A.K., Casewit C.J., Colwell K.S., et al. (1992). UFF, A full periodic-table force-field for molecular mechanics and molecular dynamics simulations. Journal of American Chemical Society 114, 10024–10035.

Xu K.-Y., Aifantis E.C., Yan Y.-H. (2008). Vibration of double-walled carbon nanotube… inner and outer tubes, Journal of Applied Mechanics, Transactions ASME, 75, 0210131–0210139.

Yakobson B.I., Brabec C.J., Bernholc J. (1996). Nanomechanics of carbon tubes: instability beyond linear response. Physical Review Letters 76, 2511–2514.